

Supporting Information

Effect of solvation on aggregation-induced luminescence of tetraphenylethene derivatives

Hui Yao,^a Meijuan Zhou,^b Xiaolong Yu,^b Ming Bai,^{a, b*}

^a Marine College, Shandong University at Weihai, Weihai 264209, People's Republic of China

^b SDU-ANU Joint Science College, Shandong University at Weihai, Weihai 264209, People's Republic of
China

E-mail: ming_bai@sdu.edu.cn

Table of Contents

Experimental Procedures

Computational methods

Fig.S1. ^1H NMR spectrum of compound **TPE-($\alpha\text{-NH}_2$)₂** in DMSO- d_6 .

Fig. S2. ^{13}C NMR spectrum of compound **TPE-($\alpha\text{-NH}_2$)₂** in DMSO- d_6 .

Fig. S3. 2D COSY spectrum of **TPE-($\alpha\text{-NH}_2$)₂** in DMSO- d_6 .

Fig. S4. ESI-MS spectrum of **TPE-($\alpha\text{-NH}_2$)₂**.

Fig. S5. Photos taken under UV irradiation of **TPE-($\alpha\text{-NH}_2$)₂**.

Fig. S6. Photos taken under UV irradiation of **TPE-($\alpha\text{-NH}_2$)₂** in different water-THF fractions.

Fig. S7. FL and absorption spectra of **TPE-($\alpha\text{-NH}_2$)₂** in different solvents-water mixtures.

Fig. S8. FL and absorption spectra of **TPE-($\alpha\text{-NH}_2$)₂** in different solvents-water mixtures with ultrasound.

Fig. S9. Fluorescence spectra of **TPE-($\alpha\text{-NH}_2$)₂** in the water-acetonitrile.

Fig. S10. FL spectra of **TPE-($\alpha\text{-NH}_2$)₂** in the water-THF mixture ($f_w = 90\%$) over time.

Fig. S11. SEM pictures of **TPE-($\alpha\text{-NH}_2$)₂** suspensions in the water-THF mixture ($f_w = 90\%$).

Fig. S12. SEM pictures of **TPE-($\alpha\text{-NH}_2$)₂** suspensions in the other solvents-mixture ($f_w = 90\%$).

Fig. S13. XRD patterns of **TPE-($\alpha\text{-NH}_2$)₂**.

Fig. S14. The optimized structures of the combinations of **TPE-($\alpha\text{-NH}_2$)₂**-Solvent- H_2O .

Fig. S15. The time-resolved emission decay curves of **TPE-($\alpha\text{-NH}_2$)₂** in the THF-water mixture.

Fig. S16 The stacking structure of **TPE-($\alpha\text{-NH}_2$)₂**-THF- H_2O .

Table S1 The fluorescence quantum efficiency and fluorescence lifetime data of **TPE-($\alpha\text{-NH}_2$)₂** in the THF-water mixture.

Table S2. Crystallographic data of **TPE-($\alpha\text{-NH}_2$)₂**.

Table S3. The binding energies for the combinations of **TPE-($\alpha\text{-NH}_2$)₂**-Solvent- H_2O using the density functional M06-2X (Gas phase)

Table S4. Optimized structures and geometric parameters for **TPE-($\alpha\text{-NH}_2$)₂** using the density functional M06-2X compared with crystal **TPE-($\alpha\text{-NH}_2$)₂**.

Notes and references

Experimental Section

General Remarks. Toluene was distilled from CaH₂ under nitrogen. Column chromatography was carried out on a silica gel column (Qingdao Haiyang, 200-300 mesh) with the indicated eluents. All the other reagents such as diphenylketone, carbon tetra bromide, triphenyl phosphine, potassium carbonate, 4-aminobenzeneboronic acid hydrochloride, 2-aminobenzeneboronic acid hydrochloride and tetra (triphenyl phosphine) palladium were purchased from Energy Chemical company and used as received. Tetrahydrofuran, acetone, 1,4-dioxane, dimethylformamide, dimethylsulfoxide were spectral purity.

¹H NMR spectrum was recorded on a Bruker DPX 400 spectrometer (¹H: 400 MHz, ¹³C: 100 MHz) in DMSO-*d*₆. Spectra were referenced internally using the residual solvent resonances (δ = 3.30 ppm, 2.50 ppm for ¹H NMR) relative to SiMe₄ (δ = 0 ppm). ¹³C NMR spectrum was referenced internally by using the solvent resonances (δ = 39.50 ppm for DMSO-*d*₆). Electronic absorption spectra were recorded on a Hitachi U-2900 spectrophotometer (1 cm quartz cell). Five different solvents (THF, acetone, 1,4-dioxane, DMF, and DMSO) were respectively used to dissolve the **TPE-(α -NH₂)₂** to prepare five solutions of concentration 500 μ M. Solutions containing solute molecules were mixed with different proportions of water to prepare the samples to be tested. The baseline was corrected using blank control solution. Steady-state fluorescence spectra were recorded on a Hitachi F-7000 spectrophotometer using quartz cuvettes having a path length of 1 cm. The emission spectra were corrected for the wavelength dependence of the sensitivity of the detection system. ESI-MS spectrum was taken on a Thermal Fisher Q-Exactive mass spectrometer. Single crystal X-ray diffraction analyses were performed on an Agilent Super Nova Atlas Dual diffractometer using CuK α radiation (λ = 1.54184 Å). Structure was solved by direct methods using SHELXTL and refined by full-matrix least-squares on F² using SHELX-97. Hydrogen atoms were placed in calculated positions with isotropic displacement parameters set to 1.2 \times U_{eq} of the attached atom. The X-ray crystallographic intensity data was about the suspended solids centrifuged from THF-water mixture with ultrasound treatment. Scanning electron microscopy (SEM) images were performed on a HITACHI TM-4000 Plus microscope operated at an accelerating voltage of 15.0 kV. The particle size was measured by a Zetasizer Nano ZS (Malvern Instruments Ltd., Worcestershire, UK) through the dynamic laser scattering (DLS) method at 25 °C.

Crystallographic data (excluding structure factors) for the structure reported in this paper has been deposited in the Cambridge Crystallographic Data Center with CCDC Number: 2119650

Synthesis of compound 1,1-dibromo-tilbene, DBT-Br

Benzophenone (1.82 g, 10 mmol), carbon tetra bromide (6.63 g, 20 mmol) and triphenylphosphine (10.49 g, 40 mmol) were placed in a 250 mL round-bottomed flask, and 150 mL dry toluene was added under the protection of nitrogen. The flask was heated to 130

°C. After refluxing for 4 days, the reaction was cooled to room temperature. The solution was evaporated and then the crude product was carried out column chromatography with *n*-hexane as the mobile phase to obtain 1.11 g light yellow solid with a yield of 61.1 %.

Synthesis of 1,1-Bis (2-Aminophenyl)-2,2-Diphenylethylene, [TPE-(α -NH₂)₂]

1,1-dibromo-tilbene (0.338 g, 1 mmol), 2-aminobenzeneboronic acid hydrochloride (0.867 g, 5 mmol), potassium carbonate (0.76 g, 5.5 mmol) and tetras(triphenylphosphine) palladium (0.115 g, 0.1 mmol) were placed in a 50 mL round-bottomed flask 25 mL toluene was added under the protection of nitrogen. After dissolution, 0.5 mL water and 0.5 mL ethanol were added. The reaction was stirred at 110°C for 12 h. Then the reaction was cooled down and the solvent was evaporated. The reaction was extracted with dichloromethane (3×50 mL). The organic phase was combined, dried with anhydrous magnesium sulfate and concentrated under reduced pressure. Using *n*-hexane/dichloromethane (75/25, v/v) as mobile phase for column chromatography, 0.191 g white solid was obtained with a yield of 56.5 %. ¹H NMR (400 MHz, DMSO-*d*₆), (TMS, ppm): 7.07 (m, 10H, *J* = 2.9 Hz, ArH); 6.84 (dd, 4H, *J* = 1.3 Hz, ArH); 6.43 (m, 4H, *J* = 1.0 Hz, ArH); 4.67 (d, 4H, *J* = 0.8 Hz, -NH₂). ¹³C NMR (100 MHz, DMSO-*d*₆), δ : 144.94, 142.60, 142.39, 136.08, 130.60, 129.82, 127.48, 127.43, 127.08, 126.70, 116.31, 114.86. ESI-MS: [M+H⁺] actual value is 363.476; The theoretical value of C₂₆H₂₃N₂ is 363.476.

Computational methods

In this study, DFT¹ calculations were performed to obtain detailed information on the interactions between **TPE-(α -NH₂)₂** and each of the five molecules (THF, acetone, 1,4-dioxane, DMF, and DMSO) as well as between H₂O molecule and each of the five molecules. We used the SMD continuum solvation model² as implemented in the Gaussian 16 program package.³ Water was chosen as solvent in the SMD calculations. All of the structures in this work were optimized using the M06-2X⁴ density functional in conjunction with 6-311++G(d, p) basis sets for all the atoms. The M06-2X functional gives a realistic structure of **TPE-(α -NH₂)₂** when comparing with the geometric parameters of crystalline **TPE-(α -NH₂)₂** as shown in Table S4, ESI†. BSSE calculations⁵ were performed in gas phase (Table S3, ESI†). For the solvent phase, the BSSE corrected binding energies were obtained using the corrections from the gas phase (Table 1).

The DFT calculations were performed using Vienna ab initio Simulation Package (VASP) to optimize the stacking-structure of **TPE-(α -NH₂)₂**-THF-H₂O (Fig. S16). It includes two **TPE-(α -NH₂)₂** molecules, one THF molecule, and thirty-three H₂O molecules in the stacking-structure of **TPE-(α -NH₂)₂**-THF-H₂O. This stacking-structure is placed in a big cubic cell with the lattice constant of 30.0 Å × 30.0 Å × 30.0 Å. The energy cutoff for the plane-waves was set to 500 eV.

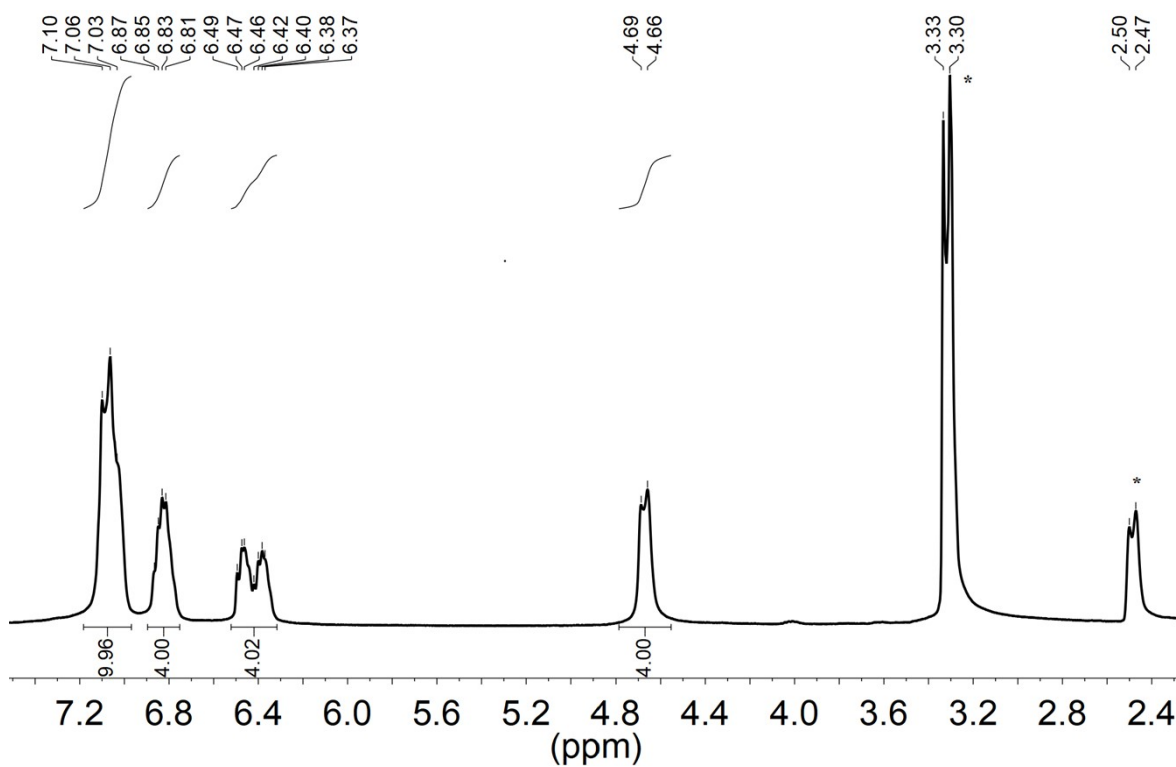


Figure S1. ^1H NMR spectrum of compound $\text{TPE}-(\alpha\text{-NH}_2)_2$ in $\text{DMSO-}d_6$. The residual solvent signals are marked with asterisks.

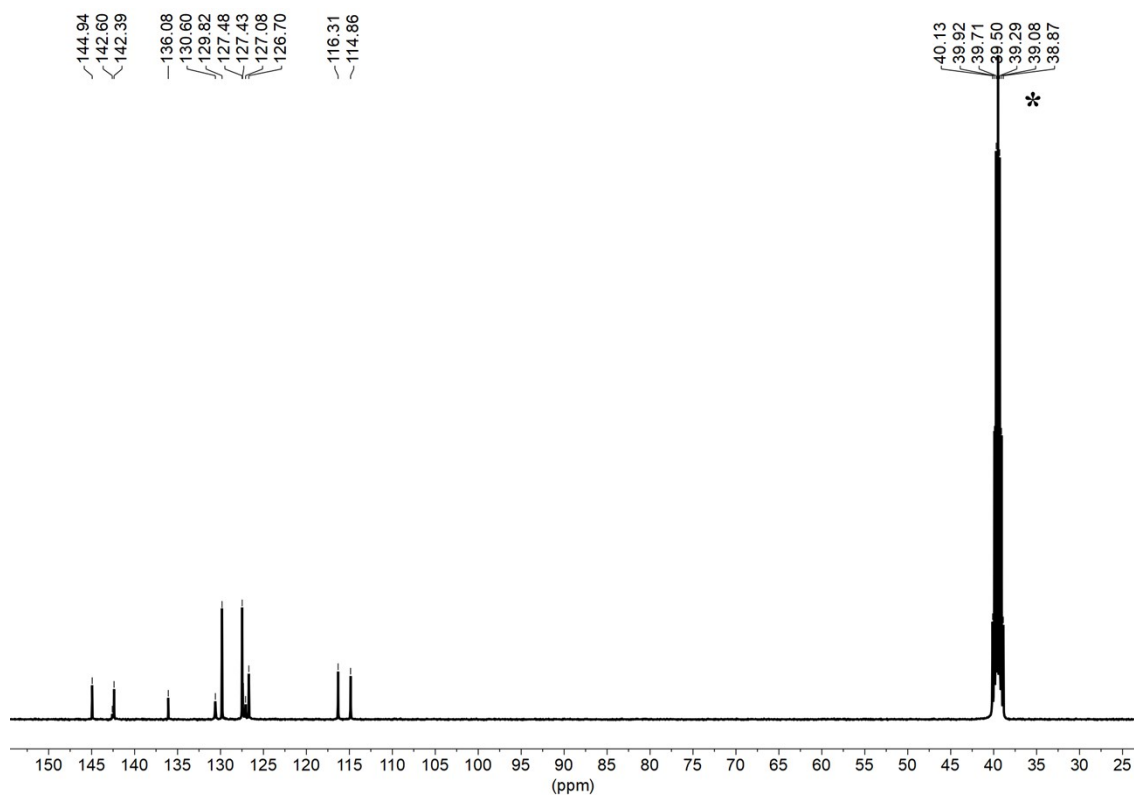


Figure S2. ^{13}C NMR spectrum of compound $\text{TPE}-(\alpha\text{-NH}_2)_2$ in $\text{DMSO-}d_6$.

The residual solvent signals are marked with asterisks.

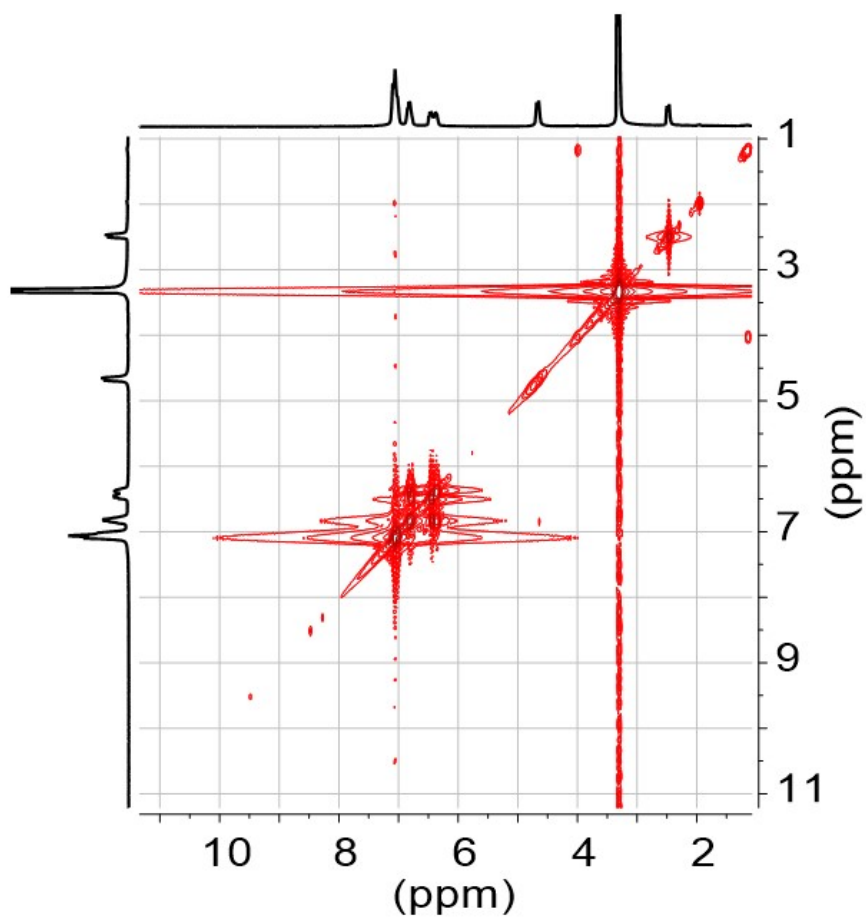


Figure S3. 2D COSY spectrum of TPE-(α -NH₂)₂ in DMSO-*d*₆.

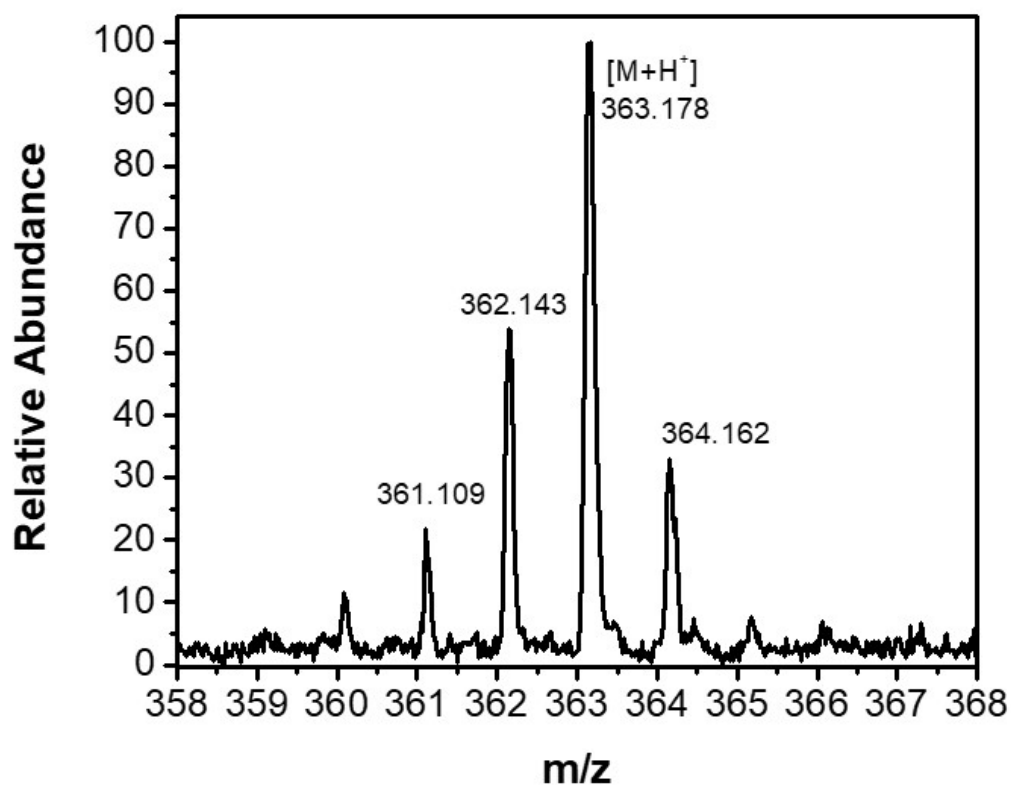


Figure S4. ESI-MS spectrum of TPE-(α -NH₂)₂.

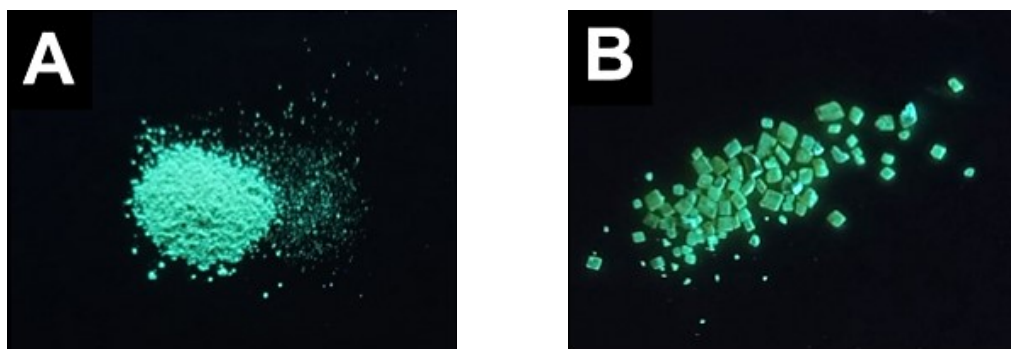


Figure S5. Photos of $\text{TPE}-(\alpha\text{-NH}_2)_2$ taken under UV irradiation (365 nm). (A) solid powder (B) crystals.

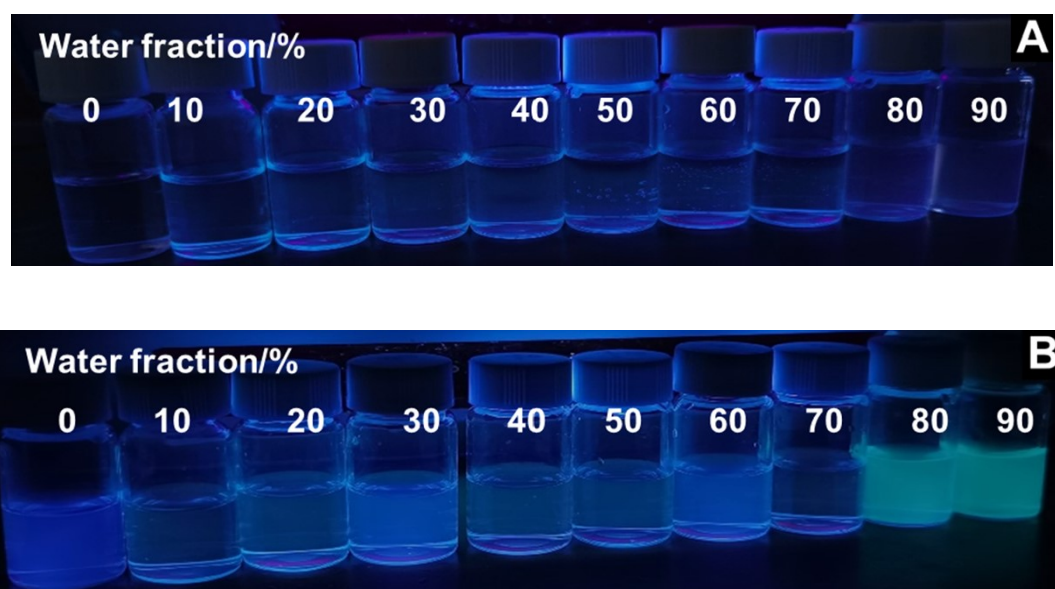


Figure. S6. Photos of $\text{TPE}-(\alpha\text{-NH}_2)_2$ in different water-THF fractions taken under UV (365 nm) irradiation. (A) Non-ultrasonic conduction (B) Ultrasonic conduction.

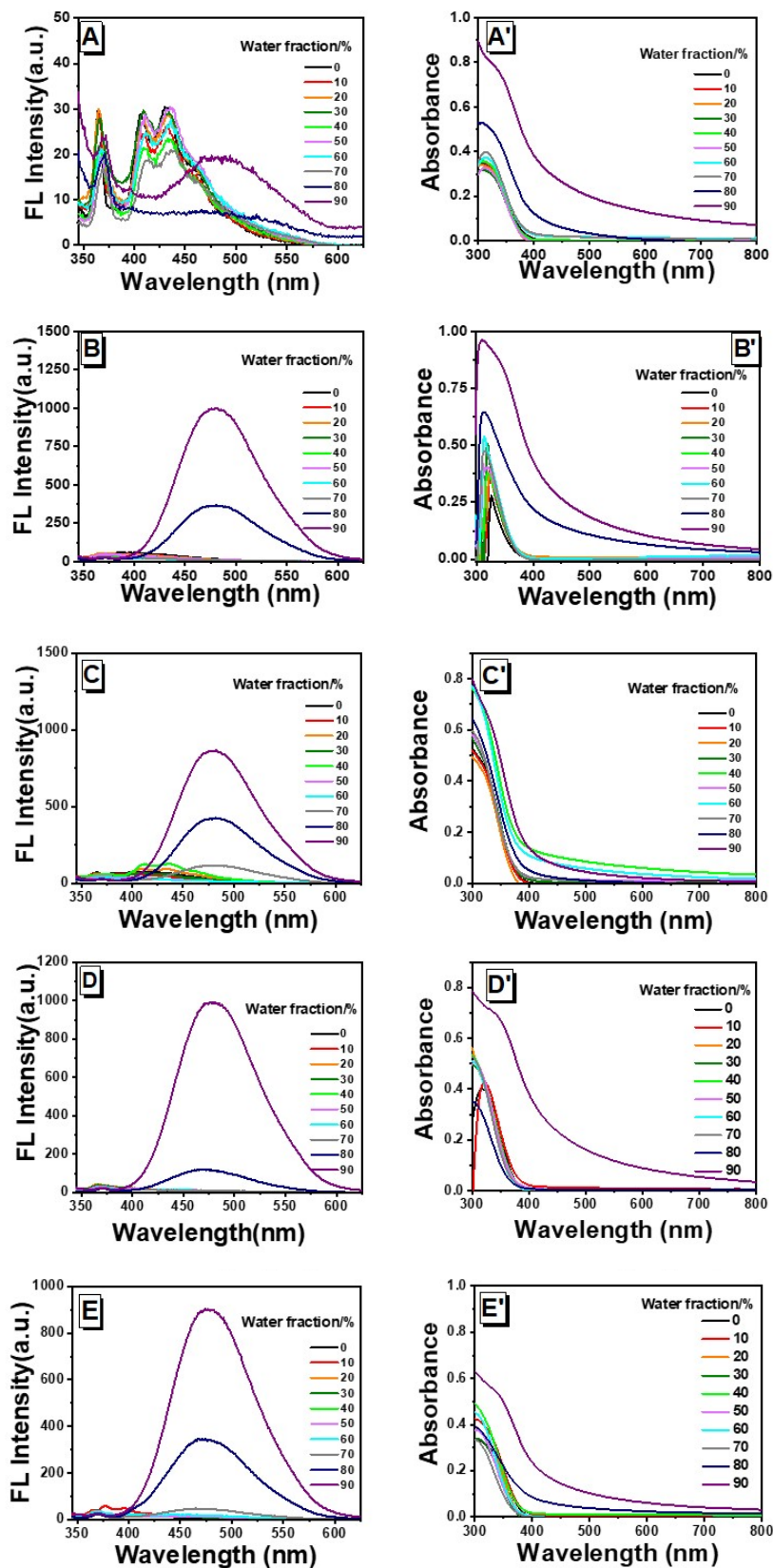


Figure S7. Fluorescence and absorption spectra of $\text{TPE}-(\alpha\text{-NH}_2)_2$ in the water-THF (A, A'), water-acetone (B, B'), water-1,4-dioxane (C, C'), water-DMF (D, D') and water-DMSO (E, E') mixtures with different water fractions. $C = 50 \mu\text{M}$; λ_{ex} : 330 nm (5 nm, 5 nm); 293 K.

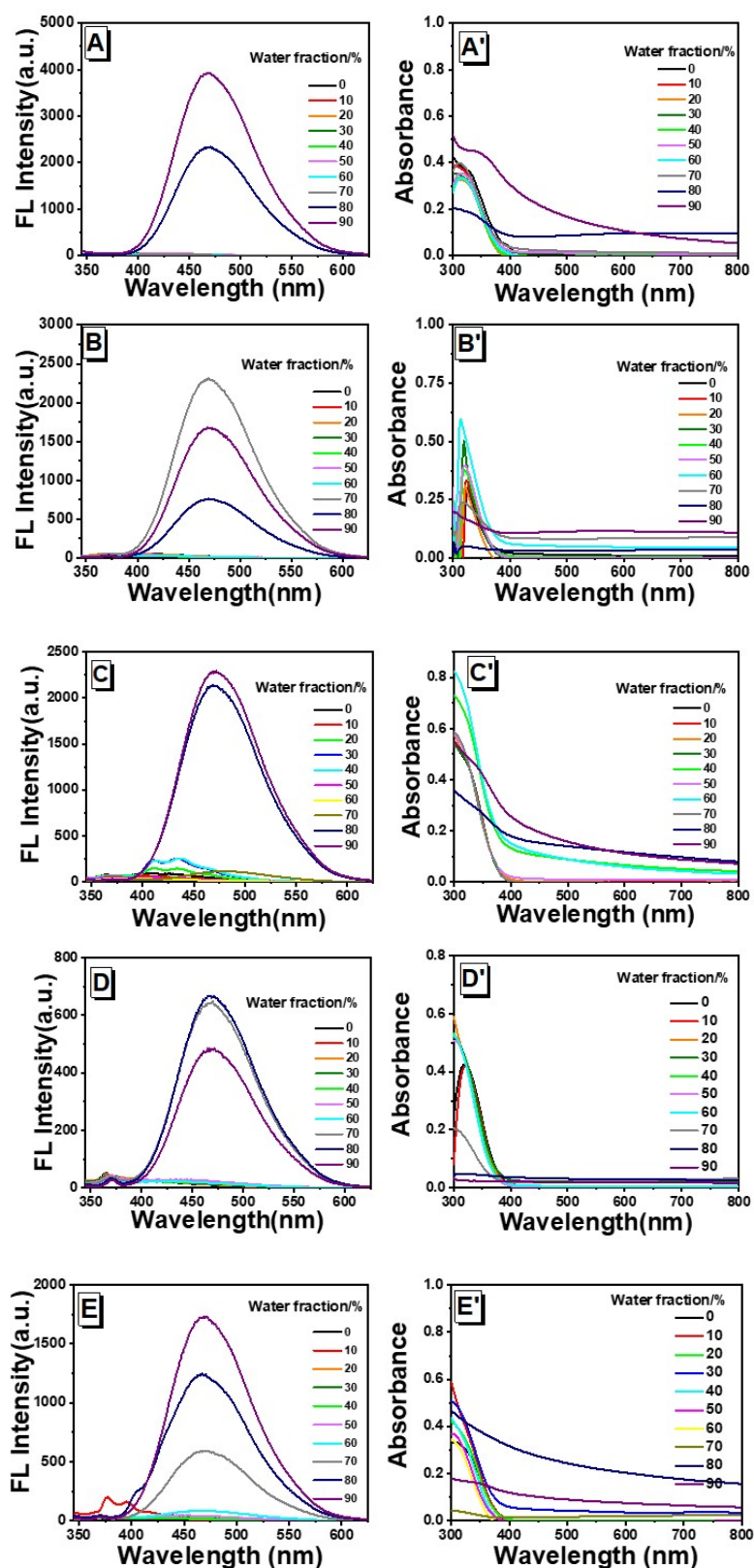


Figure S8. Fluorescence and absorption spectra of **TPE-(α -NH₂)₂** in the water-THF (A, A'), water-acetone (B, B'), water-1,4-dioxane (C, C'), water-DMF (D, D') and water-DMSO (E, E') mixtures with different water fractions. ultrasonic conduction-40 kHz, 200 W, 2 min; C = 50 μ M; λ_{ex} : 330 nm (5 nm, 5 nm); 293 K.

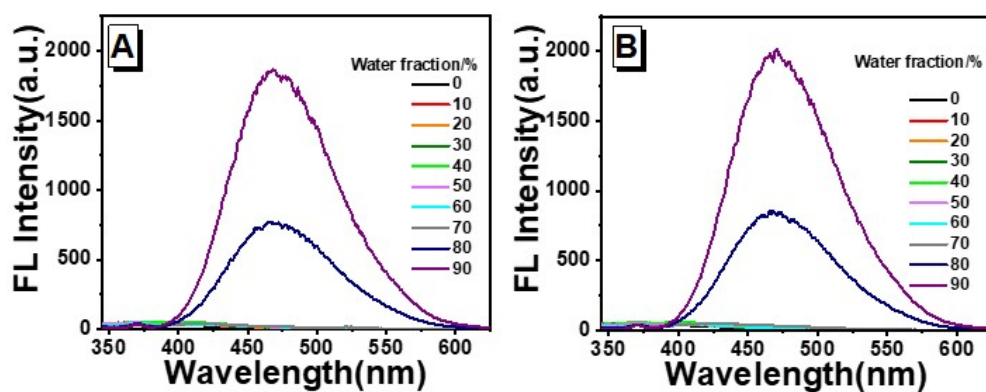


Figure S9. Fluorescence spectra of TPE-(α -NH₂)₂ in the water-acetonitrile. (A) Non-ultrasonic conduction (B) Ultrasonic conduction.

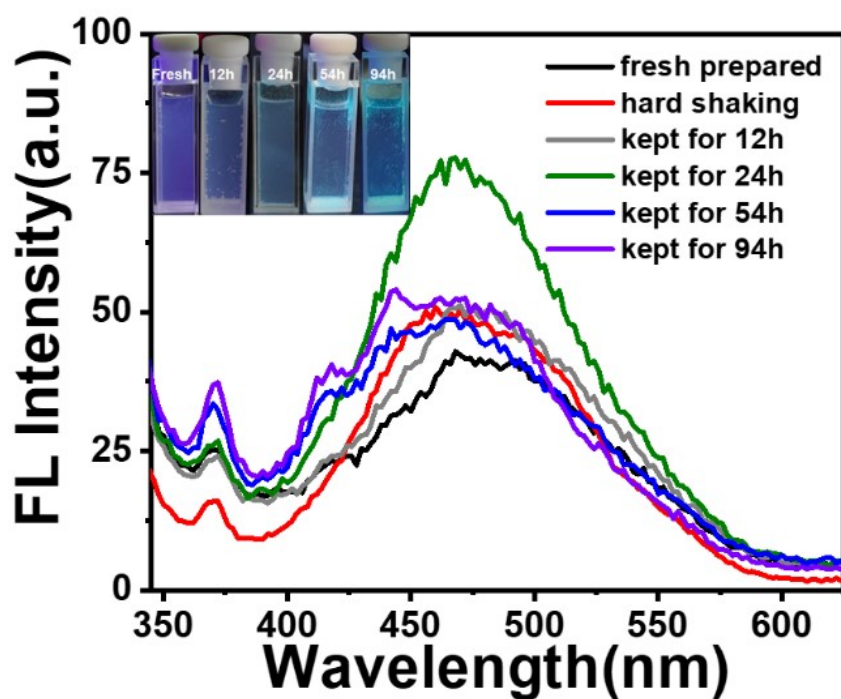


Figure S10. Fluorescence spectra of TPE-(α -NH₂)₂ in the water-THF mixture ($f_w = 90\%$) over time, and an inserted photograph taken under the UV (365 nm) irradiation.

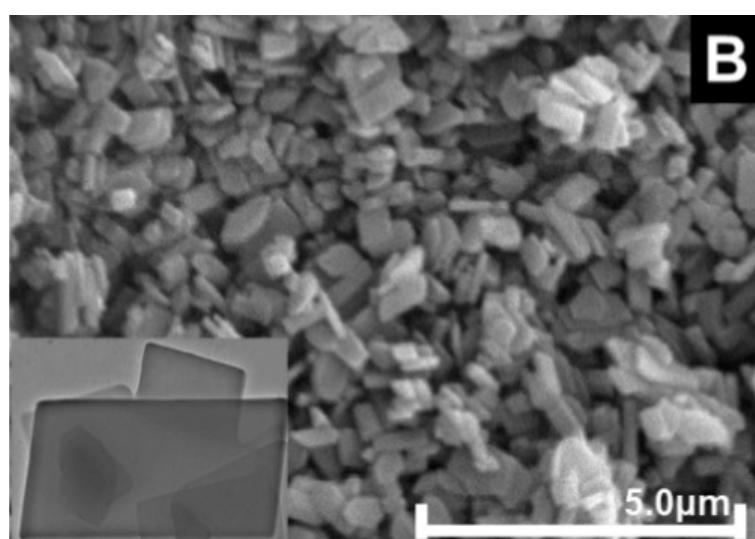
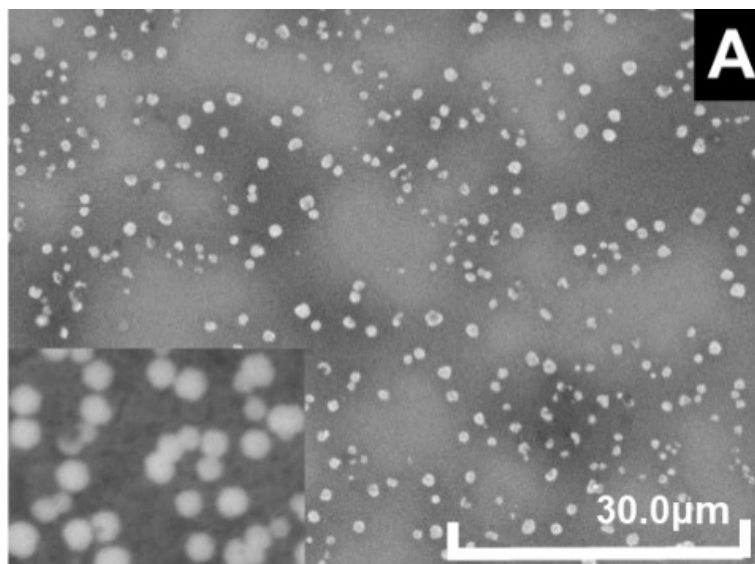


Figure S11. SEM pictures of $\text{TPE}-(\alpha\text{-NH}_2)_2$ suspensions in the water-THF mixture ($f_w = 90\%$). (A) Non-ultrasonic conduction, picture in the left bottom is with high magnification. (B) Ultrasonic conduction, left bottom is TEM picture.

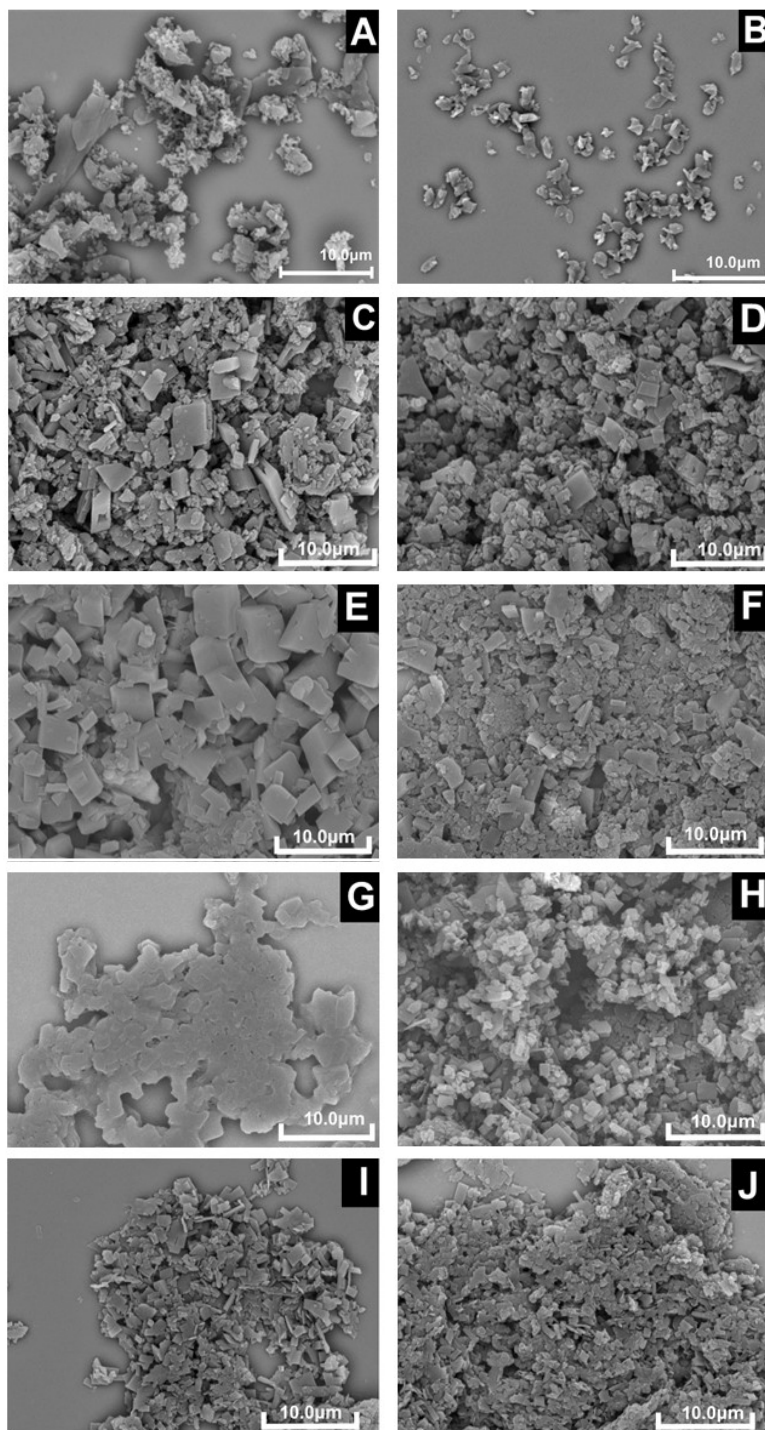


Figure S12. SEM pictures of **TPE-(α -NH₂)₂** suspensions water-acetone (A, B), water-1,4-dioxane (C, D), water-DMF (E, F), water-DMSO (G H) mixtures and water-acetonitrile (I, J) without (A, C, E, G, I) and with (B, D, F, H, J) ultrasonic conduction. ($f_w = 90\%$).

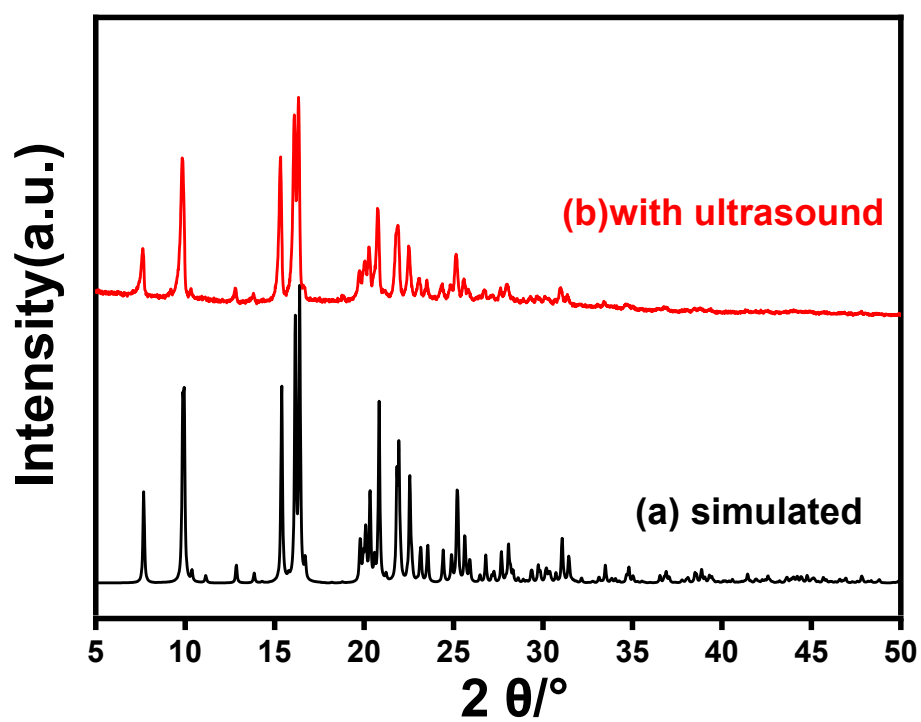


Figure S13. XRD patterns of TPE-(α -NH₂)₂: (a) simulated pattern of the single crystal; (b) samples of suspensions in water-THF mixture after ultrasonication ($f_w = 90\%$).

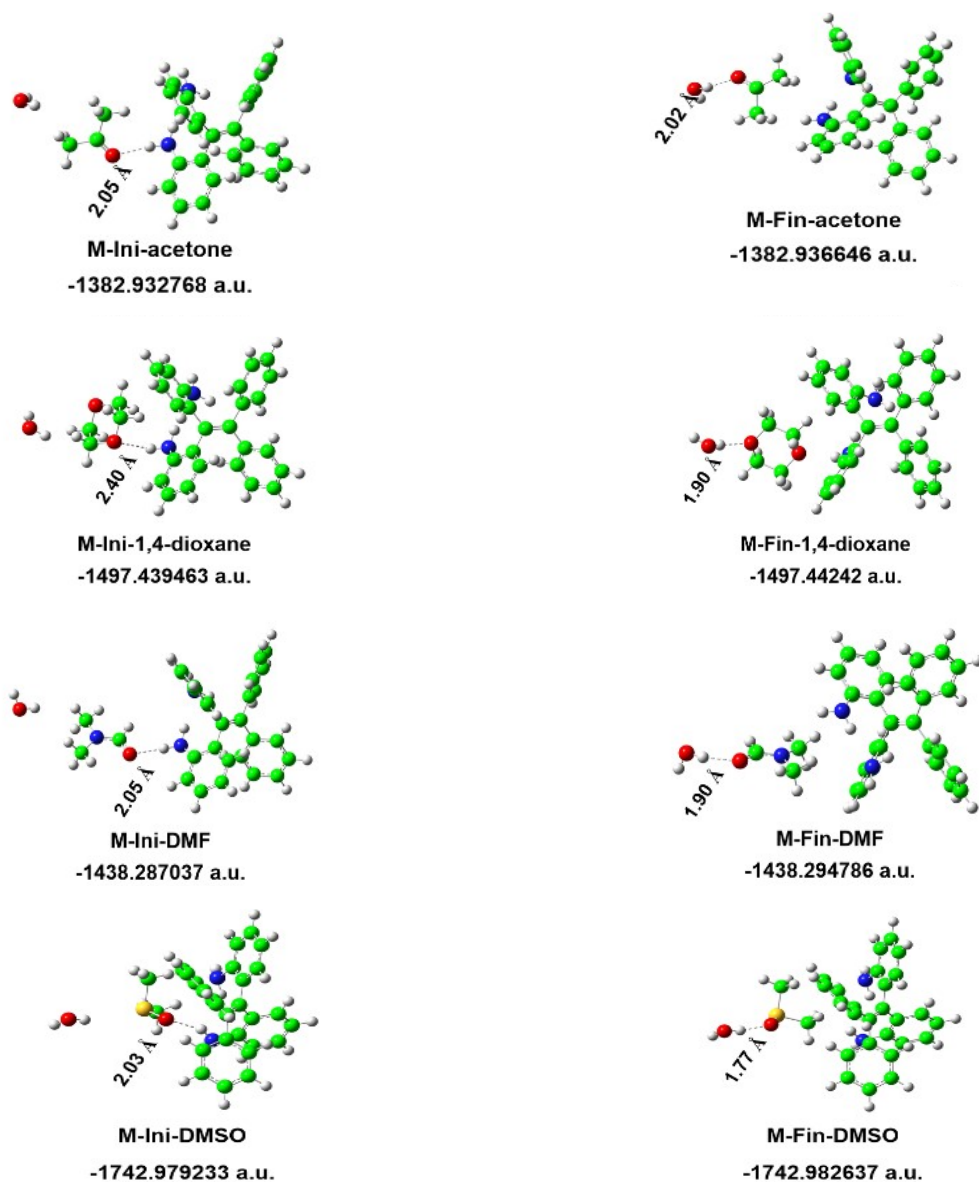


Figure S14. The optimized structures of the combinations of **TPE-(α -NH₂)₂**-Solvent-H₂O. (Solvent: acetone, 1,4-dioxane, DMF, and DMSO) as found using M06-2X (M) in SMD-water model. In the structures Ini, the solvent molecule is closer to the **TPE-(α -NH₂)₂** molecule than the H₂O molecule. In the structures of Fin, the solvent molecule is closer to the H₂O molecule than the **TPE-(α -NH₂)₂** molecule. C: green, O: red, H: white, N: blue. Black numbers around the dotted lines represent the distances between H and O for the weak hydrogen bonds. The black numbers at the bottom of each structure represent the total energy

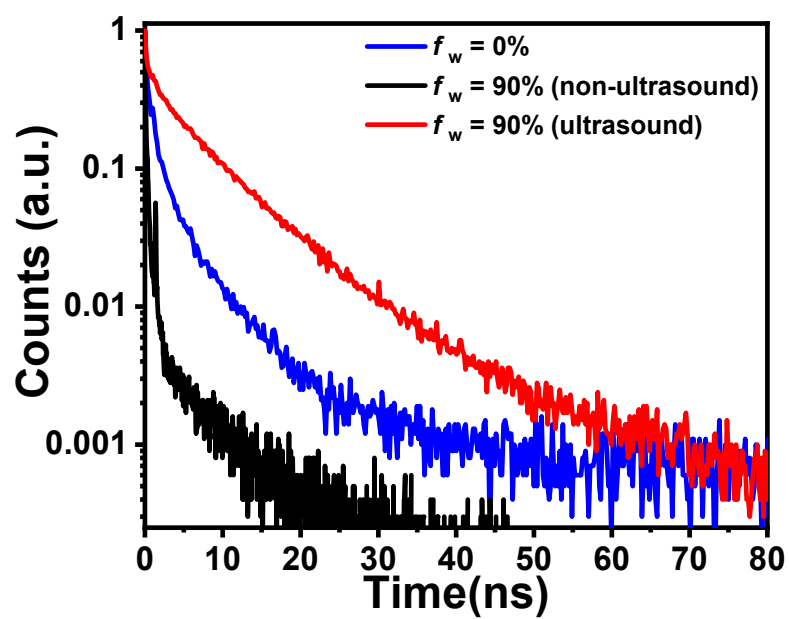


Figure S15 The time-resolved emission decay curves (λ_{ex} :330 nm) of TPE-(α -NH₂)₂ in the THF-water mixture.

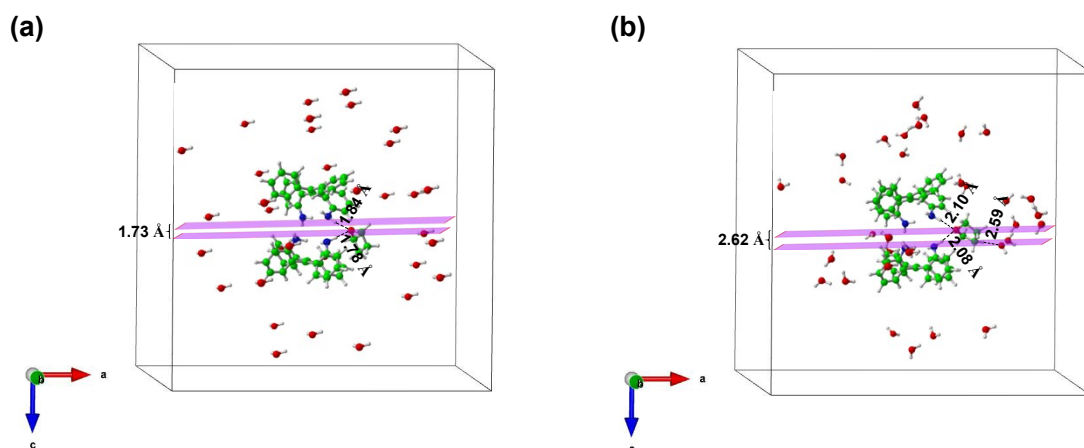


Figure S16. The stacking-structure* of **TPE-(α -NH₂)₂**-THF-H₂O (a) without relaxation and (b) with relaxation (C: green, O: red, H: white, N: blue. Black numbers around the dotted lines represent the weak hydrogen bonds' length).

* In Fig. S16(a), thirty-three H₂O molecules are randomly placed around the two **TPE-(α -NH₂)₂** molecules and one THF molecule. The distance between the two **TPE-(α -NH₂)₂** molecules is approximately 1.76 Å. After structural relaxation, THF molecule is a little further away from the two **TPE-(α -NH₂)₂** molecules. However, there are still two weak hydrogen-bonds formed between the O atom of THF molecule and N atom of -NH₂ group of **TPE-(α -NH₂)₂** molecule. The thirty-three H₂O molecules have been rearranged due to the formation of intermolecular hydrogen bonds. Only one H₂O molecule gets closer to the THF molecule and forms one weaker hydrogen-bond with THF molecule. In addition, the distance between the two **TPE-(α -NH₂)₂** molecules is about 2.62 Å, which is 0.86 Å larger than that in the initial structure of Fig. S16(a). In the relaxed stacking-structure of **TPE-(α -NH₂)₂**-THF-H₂O, the two **TPE-(α -NH₂)₂** molecules will keep the distance from each other when there are weak interactions between them and THF molecules.

Table S1 The fluorescence quantum efficiency and fluorescence lifetime data of **TPE-(α -NH₂)₂** in the THF-water mixture.

TPE-(α -NH ₂) ₂ in the THF-water	Φ_F (%)	Fluorescence Lifetime			
		τ_1 (ns)	A ₁	τ_2 (ns)	A ₂
$f_w = 0\%$	1.64	1.03	83%	5.96	17%
$f_w = 90\%$ (non-ultrasound)	2.26	0.02	82%	0.28	18%
$f_w = 90\%$ (ultrasound)	71.26	2.94	38%	9.73	62%

Table S2 Crystallographic data of **TPE-(α -NH₂)₂**.

Temperature (K)	293 (2)
Chemical formula	C ₂₆ H ₂₂ N ₂
Wavelength	1.54184
Crystal system	Triclinic
space group	<i>P</i> -1
Formula weight	362.46
Unit cell dimensions	a (Å) 9.1788 (6) b (Å) 9.5316 (6) c (Å) 12.5301 (9) α (°) 70.240 (6) β (°) 75.746 (6) γ (°) 83.129 (5)
Volume (Å ³)	999.12 (12)
Z	2
D _c (g cm ⁻³)	1.592
F (000)	479
μ (mm ⁻¹)	1.757
R ₁ , [I > 2 σ (I)]	0.0547
R ₁ , (all data)	0.0621
wR ₂ , [I > 2 σ (I)]	0.1552
ω R ₂ , (all data)	0.1655
GOF	1.040

Table S3 The binding energies (kcal/mol) for the combinations of **TPE-(α -NH₂)₂**-
Solvent-H₂O using the density functional M06-2X (Gas phase) *

System	ΔE_{Ini}^{Raw}	$\Delta E_{Ini,gas}^{BSSE\ corrected}$	ΔE	$\Delta E_{Fin,gas}^{BSSE\ corrected}$	$\Delta E_{Ini-Fin}^{Raw}$	$\Delta E_{Ini-Fin,gas}^{BSSE\ corrected}$
T-THF-H ₂ O	9.82	8.64	8.78	7.71	1.04	0.93
T-Acetone-H ₂ O	4.56	3.80	7.64	6.78	-3.08	-2.98
T-1,4-Dioxane-H ₂ O	8.77	7.31	14.79	13.09	-6.02	-5.78
T-DMF-H ₂ O	4.99	4.45	13.10	12.16	-8.11	-7.71
T-DMSO-H ₂ O	11.42	9.03	11.34	8.98	0.08	0.05

*: (1) Ini and Fin, i.e., the combination of T-Solvent-H₂O [*T*: **TPE-(α -NH₂)₂**; solvent: THF, acetone, 1,4-dioxane, DMF and DMSO].

(2) In the Ini structure of T-Solvent-H₂O, the distance between *T* and solvent is shorter than that between H₂O and solvent and one weak hydrogen bond is formed between the hydrogen atom of the -NH₂ group of *T* and the oxygen atom of solvent. In the Fin structure of T-Solvent-H₂O, the distance between H₂O and solvent is smaller than that between *T* and solvent and one weak hydrogen bond is formed between the hydrogen atom of H₂O and the oxygen atom of solvent.

(3) BSSE: Basis Set Superposition Error.

For the gas phase, ΔE_{Ini}^{Raw} and ΔE_{Fin}^{Raw} represent the total energy of Ini structure and Fin structure without

the BSSE correction in the gas phase, respectively. $\Delta E_{Ini-Fin}^{Raw} = \Delta E_{Ini}^{Raw} - \Delta E_{Fin}^{Raw}$

$\Delta E_{Ini}^{BSSE\ corrected}$ and $\Delta E_{Fin}^{BSSE\ corrected}$ represent the relative total energy of the Ini structure and Fin structure with the BSSE correction in the gas phase, respectively.

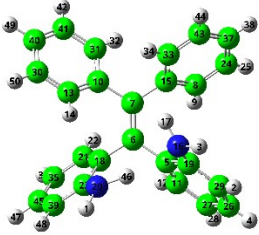
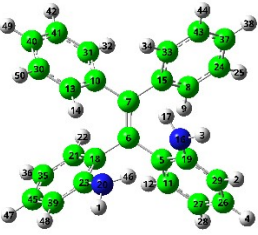
$$\Delta E_{Ini-Fin}^{BSSE\ corrected} = \Delta E_{Ini}^{BSSE\ corrected} - \Delta E_{Fin}^{BSSE\ corrected}$$

(4) For the solvent phase (**Table 1**), $\Delta E_{Ini,sol}^{BSSE\ corrected} = \Delta E_{Ini} - (\Delta E_{Ini}^{Raw} - \Delta E_{Ini,gas}^{BSSE\ corrected})$,

$$\Delta E_{Fin,sol}^{BSSE\ corrected} = \Delta E_{Fin} - (\Delta E_{Fin}^{Raw} - \Delta E_{Fin,gas}^{BSSE\ corrected}), \Delta E_{Ini-Fin} = \Delta E_{Ini} - \Delta E_{Fin},$$

$$\Delta E_{Ini-Fin,sol}^{BSSE\ corrected} = \Delta E_{Ini,sol}^{BSSE\ corrected} - \Delta E_{Fin,sol}^{BSSE\ corrected}$$

Table S4 Optimized structures and geometric parameters for **TPE-(α -NH₂)₂** using the density functional M06-2X compared with crystal **TPE-(α -NH₂)₂**.

	
TPE-(α-NH₂)₂ (crystal)	TPE-(α-NH₂)₂ (M06-2X) -1113.365421 Hartree
¹ d (C ⁶ -C ⁷) = 1.35 Å	¹ d (C ⁶ -C ⁷) = 1.35 Å
² D (C ¹⁰ -C ⁷ -C ⁶ -C ⁵) = -174.2°	² D (C ¹⁰ -C ⁷ -C ⁶ -C ⁵) = -174.5°
² D (C ¹⁵ -C ⁷ -C ⁶ -C ¹⁸) = -171.2°	² D (C ¹⁵ -C ⁷ -C ⁶ -C ¹⁸) = -171.3°
³ A (C ⁵ -C ⁶ -C ¹⁸) = 114.9°	³ A (C ⁵ -C ⁶ -C ¹⁸) = 114.8°
³ A (C ¹⁰ -C ⁷ -C ¹⁵) = 114.2°	³ A (C ¹⁰ -C ⁷ -C ¹⁵) = 115.7°

C: green, H: white, N: blue.

¹d represents the length of C=C;

²D represents the dihedral angle;

³A represents the angle.

Notes and references

1. C. H. Choi and M. Kertesz, *J. Phys. Chem. A*, 1997, **101**, 3823-3831.
2. A. V. Marenich, C. J. Cramer and D. G. Truhlar, *J. Phys. Chem. B*, 2009, **113**, 6378-6396.
3. M. J. Frisch, G. W. Trucks, H. B. Schlegel, G. E. Scuseria, M. A. Robb, J. R. Cheeseman, G. Scalmani, V. Barone, G. A. Petersson, H. Nakatsuji, X. Li, M. Caricato, A. V. Marenich, J. Bloino, B. G. Janesko, R. Gomperts, B. Mennucci, H. P. Hratchian, J. V. Ortiz, A. F. Izmaylov, J. L. Sonnenberg, D. Williams-Young, F. Ding, F. Lipparini, F. Egidi, J. Goings, B. Peng, A. Petrone, T. Henderson, D. Ranasinghe, V. G. Zakrzewski, J. Gao, N. Rega, G. Zheng, W. Liang, M. Hada, M. Ehara, K. Toyota, R. Fukuda, J. Hasegawa, M. Ishida, T. Nakajima, Y. Honda, O. Kitao, H. Nakai, T. Vreven, K. Throssell, J. A. Montgomery, Jr., J. E. Peralta, F. Ogliaro, M. J. Bearpark, J. J. Heyd, E. N. Brothers, K. N. Kudin, V. N. Staroverov, T. A. Keith, R. Kobayashi, J. Normand, K. Raghavachari, A. P. Rendell, J. C. Burant, S. S. Iyengar, J. Tomasi, M. Cossi, J. M. Millam, M. Klene, C. Adamo, R. Cammi, J. W. Ochterski, R. L. Martin, K. Morokuma, O. Farkas, J. B. Foresman and D. J. Fox, Gaussian 16, Gaussian, Inc., Wallingford CT, 2019.
4. J. Bednarko, J. Wielinska, K. Sikora, B. Liberek and A. Nowacki, *J. Comput.-Aided Mol. Des.*, 2016, **30**, 13-26.
5. Frans B. van Duijneveldt, Jeanne G. C. M. van Duijneveldt-van de Rijdt and J. H. v. Lenthe, *Chem. Rev.*, 1994, **94**, 1873-1885.